

Supporting information for:

A ruthenium tetrazole complex-based high efficiency near infrared light electrochemical cell

S1. Experimental Section

S1.1. General information

S1.1.1 Materials and instruments. All reagents and solvents in the syntheses were of reagent grade and used without further purification. (**Caution!** Sodium azide is potentially explosive and should be handled with much care.) bpy, dmbpy and phen ligands was purchased from Sigma-Aldrich and Merck.

Elemental analyses of carbon, hydrogen, and nitrogen were carried out with an Elementar Vario CHN analyzer. IR spectroscopy studies were performed on a FT-IR spectrophotometer in the 400- 4000 cm^{-1} region (w, weak; b, broad; m, medium; s, strong). ^1H NMR spectra is recorded on a Bruker 250 MHz spectrometer (s, singlet; d, doublet; t, triplet; m, multiplet; dd, double doublet). Analyses were performed. UV-vis absorption spectra in N,N dimethylformamide (DMF) solution were recorded on a 160 Shimadzu UV-vis spectrophotometer. Photoluminescence (PL) and Electroluminescence (EL) emissions spectra were recorded with an ocean optic USB 2000 spectrophotometer. Electrochemical measurements were employed in a SAMA500 electro analyzer using 10^{-3} molL^{-1} solution of acetonitrile (ACN) at a various scan rate. The electrolytic cell consists of platinum disc as the working electrode, a platinum wire as the counter electrode, and Ag/AgCl as the reference electrode. The supporting electrolyte was 0.1 molL^{-1} tetrabutylammonium perchlorate (TBAP) in DMF and ACN solutions [1]. For measuring EQE of a light emitting device, it is placed inside an integrating sphere and excited by constant current. Current or voltage is changed stepwise and each time a complete emission spectrum is taken and displayed by the software.

S1.1.2 Device fabrication and measurement: Indium tin oxide (ITO) coated glass with a sheet resistance of 20 Ω/square was used as the transparent anode. After being sufficiently cleaned by soaking in ultrasonicated isopropanol, acetone and deionized water, it was dried in the oven at 110°C for 2h. The devices were prepared by spin-coating a thin layer of each complex (SA1 and SA2) on top of an ITO glass substrate from a 5% (w/v) acetonitrile solution

at RT. All solution and film preparation were performed under ambient conditions. The thicknesses of the films were ~ 85 nm, measured with profilometry. After spincoating, the thin films were annealed at 90 °C in inert atmosphere for 14h. A Ga: In (75.5:24.5 wt %, mp 15.7 °C) eutectic as cathode (ca. 3.5 mm diameter) was printed on the top of the active layer at room temperature by using a special syringe and then connected via a thin copper wire inserted into the Ga:In contact. Finally it was sealed with epoxy cement. All EL measurement were carried out in air atmosphere. The current density, luminescence versus the voltage and emission characteristics of LEC devices were measured using an AvaSpec-125 spectrophotometer, a SAMA500 electroanalyzer system and a Photo Research PR-650 spectroradiometer.

S1.2. Synthesis and Characterization

5,6-epoxy-1,10-phenanthroline and 5-cyano-1,10-phenanthroline were synthesized according to the literature procedure [2].

5-(2H-Tetrazol-5-yl)-1,10-phenanthroline (Tzphen). The Tzphen ligand was performed according to the procedure reported by Zhang et al. from 5-cyano-1,10-phenanthroline, [3] sodium azide, and ammonium chloride in DMF except the mixture was acidified to pH=3.5. Yield: 54%. FT-IR (cm⁻¹): 3392 (m), 3069 (m), 1602 (s), 1545 (s), 1418 (w), 867 (m), 727 (w). ¹H NMR (250 MHz, DMSO): δ 9.3 (d, 1H), 9.2 (d, 1H), 8.8 (s, 1H), 8.6 (d, 1H), 8.65 (d, 1H), 7.9 (t, 1H), 7.8 (t, 1H). Anal. Calcd for C₁₃H₈N₆: C, 56.72; H, 4.03; N, 30.53. Found: C, 56.92; H, 3.64; N, 30.76.

Synthesis of Complexes SA1–SA3.

The reactions were performed under N₂ and in the absence of light. The ancillary ligands includes 2,2'-bipyridine (bpy), 4,4'-di-methyl-2,2'-bipyridine (dmbpy) and 1,10 phenanthroline (phen) for complexes SA1, SA2 and SA3, respectively.

Complex SA1: First, bpy as ancillary ligand (0.0312g, 2 mmol) was dissolved in DMF (4 mL), and then RuCl₃·3H₂O (0.026g, 1mmol) was added. The mixture was stirred and refluxed for 5 h at 140 °C under N₂. After cooling, the progress of complexation was monitored by UV-Vis. Following, the ligand Tzphen (0.032 g, 1.2 mmol) was added to prepared mixture and stirred for 5 h at 140 °C under N₂. After cooling, NaClO₄ (3 mmol) as counter ion added to mixture and stirred for 30 min. Finally, obtained red-brown solid was filtered, washed with water/ethanol

and dried (70 mg, 78% yield). ^1H NMR (DMSO) δ : 9.25 (d, 1H), 9.2 (d, 1H), 8.95 (s, 1H), 8.70–8.80 (d, 2H), 8.16 (d, 4H), 8.06 (d, 4H), 7.80–7.90 (m, 2H), 7.53 (m, 4H), 7.31 (m, 4H). ^{13}C NMR: Bpy:158.5(2C), 158(2C) (C-quaternaries), 153 (2C), 152.4 (2C) (N-ortho CHs), 138.8 (2C), 137.9(2C) N-para (CHs), 128.2, 127.2, 126.1(2C) (N-meta CHs): phen Tz ligand , 162.2 (Ct), 156.8(2C), 157.3(2C) (C-quaternaries) , 152.4 (2C) (N-ortho CHs), 135.4(2C) (N-para CHs), 126.4, 125.7 (N-meta CHs). Anal. Calcd for $\text{C}_{33}\text{H}_{24}\text{Cl}_2\text{O}_8\text{RuN}_{10}$ (860.59): C, 41.37; H, 2.94; N, 18.57%. Found: C, 41.44; H, 2.85; N, 18.49%. ESI-MS: m/z , 760. 128, $[\text{M}-\text{H}-2\text{ClO}_4]^+$.

Complex SA2: First, dmbpy was dissolved in DMF as ancillary ligands (0.0368 g, 2 mmol) and Tzphen (0.0312 g, 1.2 mmol) added to $\text{RuCl}_3 \cdot 3 \text{H}_2\text{O}$ (0.026 g, 1mmol) and according to the procedure of SA1, complex SA2 synthesized. (75 mg, 79% yield). ^1H NMR (DMSO) δ : 9.25 (d, 1H), 9.2 (d, 1H), 8.95 (s, 1H), 8.70–8.80 (d, 2H), 7.80–7.90 (d, 4H), 7.6 (m, 4H), 7.41 (m, 2H), 7.2 (d, 2H), 2.90 (s, 12H). ^{13}C NMR: Dimethyl Bpy:158.3(2C), 158.1(2C) (C-quaternaries), 153.2 (2C), 152.6 (2C) (N-ortho CHs), 128.3, 127.3, 126.2(2C) (N-meta CHs), 22.2 (2C), 22.7(2C) (CH_3): phen Tz ligand , 162.2 (Ct), 157.8(2C), 157.3(2C) (C-quaternaries) , 152.1 (2C) (N-ortho CHs), 135.4(2C) (N-para CHs), 126.4, 125.7 (N-meta CHs). Anal. Calcd for $\text{C}_{37}\text{H}_{32}\text{Cl}_2\text{O}_8\text{RuN}_{10}$ (916.697): C, 41.37; H, 2.94; N, 18.57%. Found: C, 41.44; H, 2.85; N, 18.49%. ESI-MS: m/z , 816.228, $[\text{M}-\text{H}-2\text{ClO}_4]^+$.

Complex SA3: According to the procedure of SA1, complex SA3 synthesized. First, phen was dissolved in DMF as ancillary ligands (0.0368 g, 2 mmol) and Tzphen (0.0312 g, 1.2 mmol) added to $\text{RuCl}_3 \cdot 3 \text{H}_2\text{O}$ (0.026 g, 1mmol). (65 mg, 67% yield). ^1H NMR (DMSO) δ : 9.18 (d, 2H), 9.02 (d, 4H), 8.73 (d, 1H), 8.6 (s, 1H), 8.36 (d, 1H), 8.12 (d, 4H), 7.91 (d, 4H), 7.7 (m, 6H); ^{13}C NMR: Phen: 157.5 (2C), 156.5(2C), 155.2(2C), 154.5(2C) (C-quaternaries), 150.1 (2C), 149.5, 148.7 (N-ortho CHs), 137.7 (2C), 137.1 (2C) (N-para CHs), 128.1 , 127.9, 126.4(2C) (N-meta CHs), phen Tz ligand , 162.2 (Ct), 157.2(2C), 156.8(2C) (C-quaternaries) , 152 (2C) (N-ortho CHs), 135.4(2C) (N-para CHs), 126.4, 125.7 (N-meta CHs). Anal. Calcd for $\text{C}_{37}\text{H}_{24}\text{Cl}_2\text{O}_8\text{RuN}_{10}$ (908.633): C, 41.37; H, 2.94; N, 18.57%. Found: C, 41.44; H, 2.85; N, 18.49%. ESI-MS: m/z , 808.161, $[\text{M}-\text{H}-2\text{ClO}_4]^+$.

S2. ^1H NMR and ^{13}C NMR spectra:

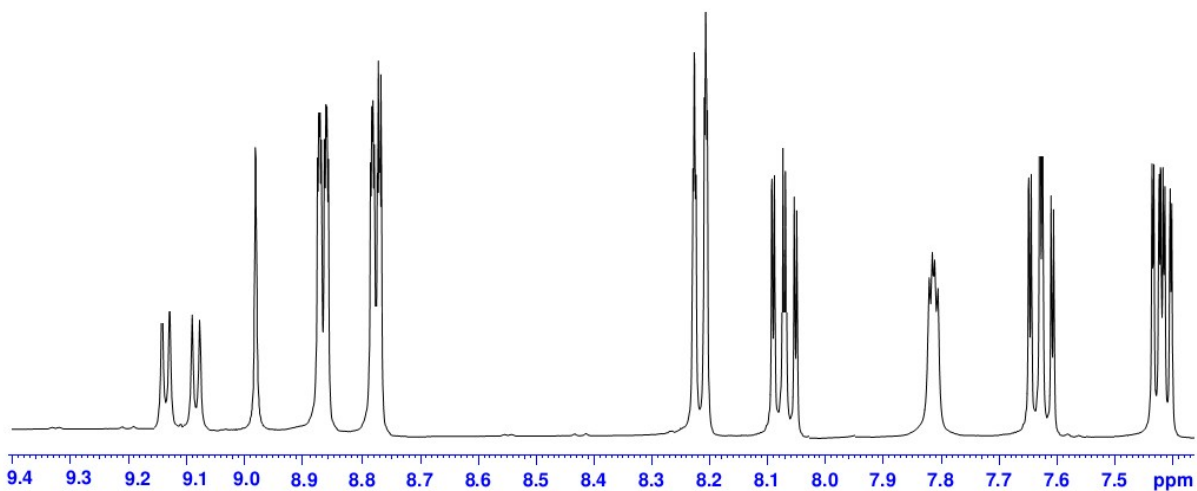


Figure S1. Aromatic region of ¹H NMR spectra (400MHz) of complex (SA1) in DMSO-d₆ at RT.

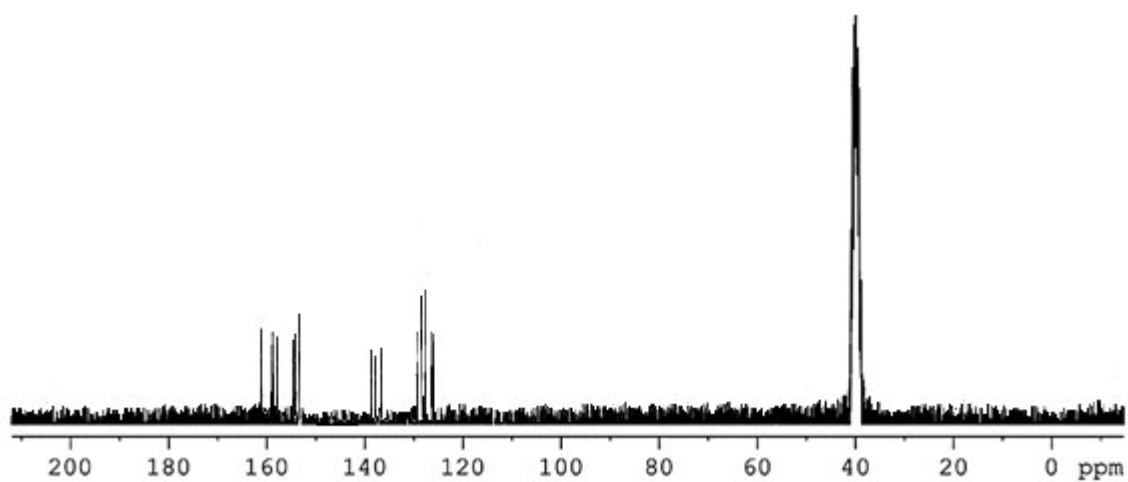


Figure S2. ¹³C NMR spectra (400MHz) of complex (SA1) in DMSO-d₆ at RT.

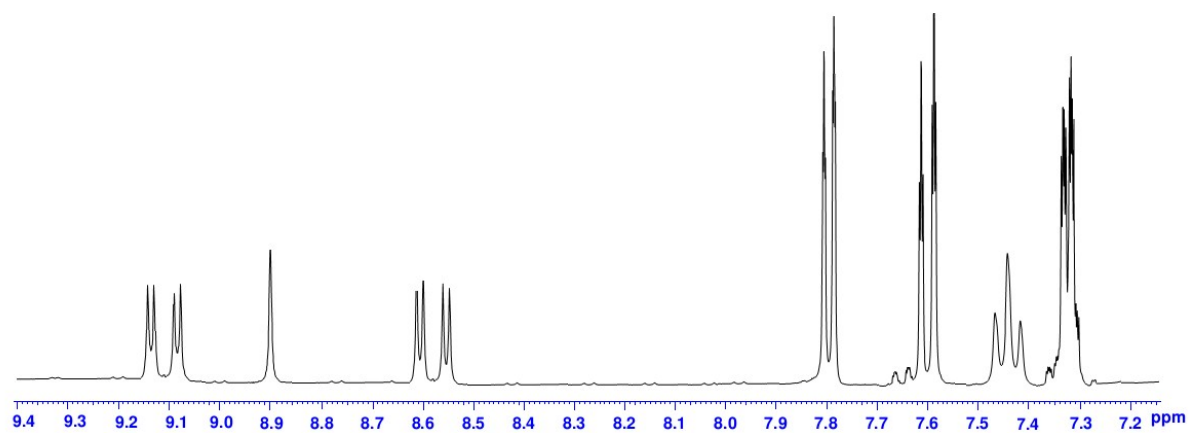


Figure S3. Aromatic region of ^1H NMR spectra (400MHz) of complex (SA2) in DMSO-d_6 at RT.

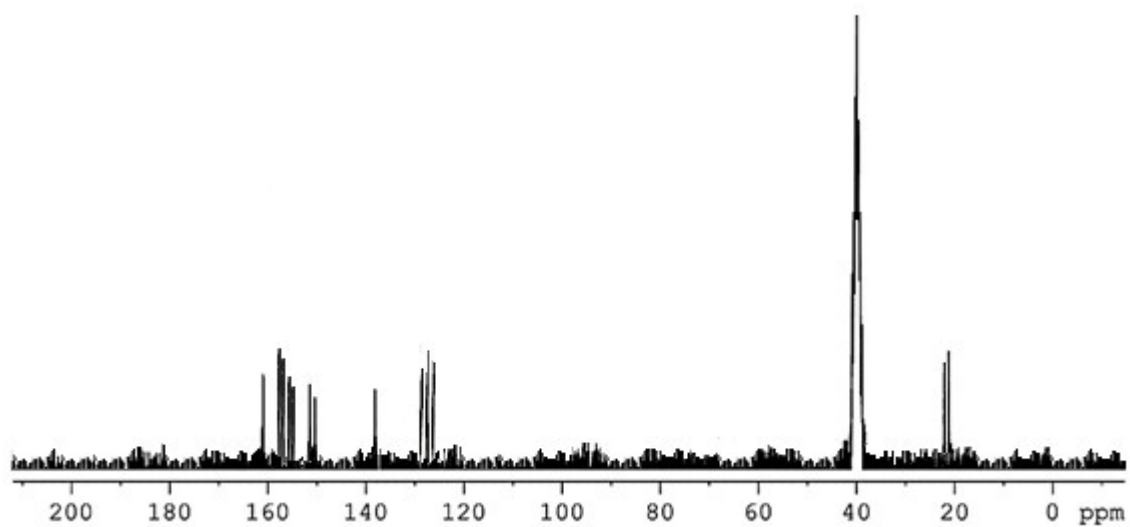


Figure S4. ^{13}C NMR spectra (400MHz) of complex (SA2) in DMSO-d_6 at RT.

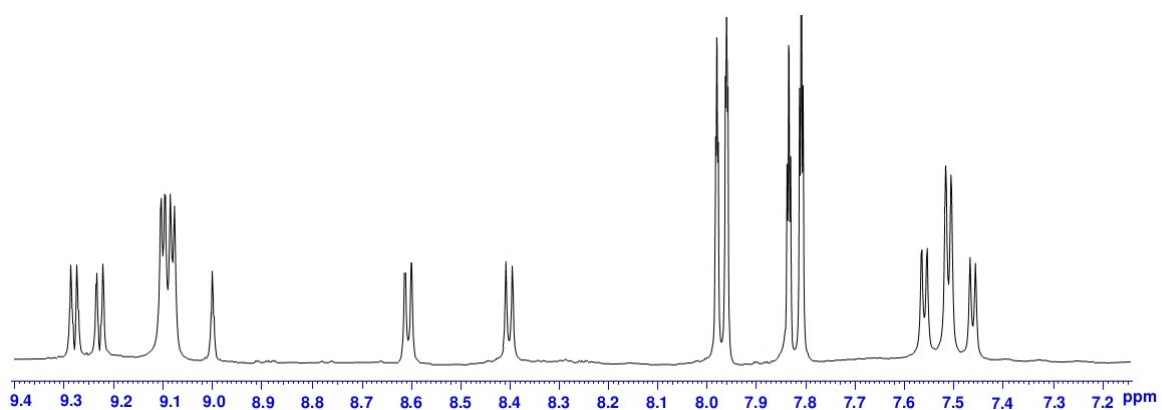


Figure S5. Aromatic region of ^1H NMR spectra (400MHz) of complex (SA3) in DMSO-d_6 at RT.

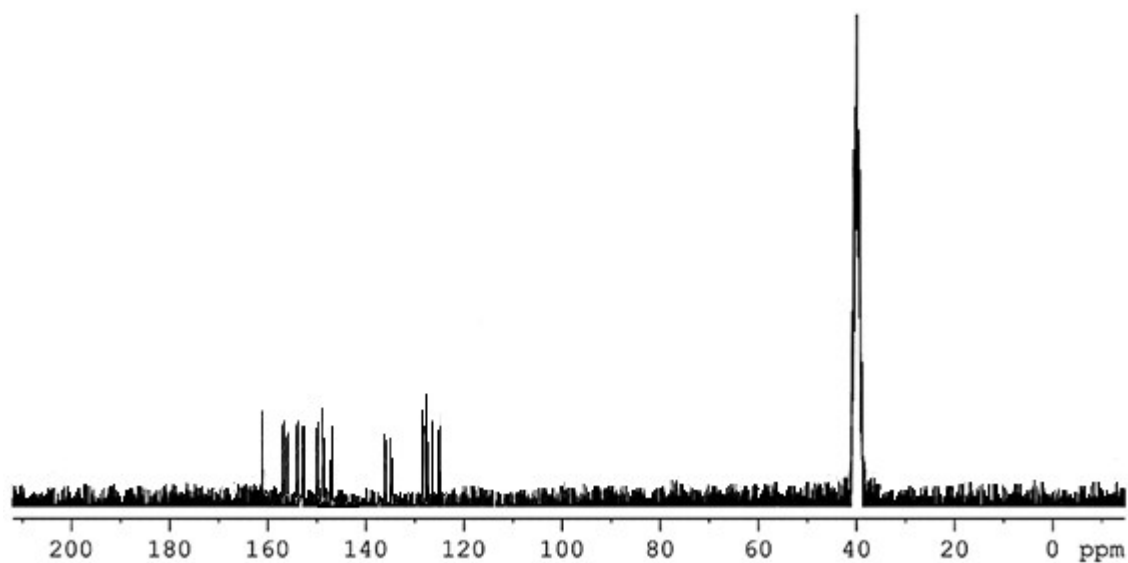


Figure S6. ^{13}C NMR spectra (400MHz) of complex (SA3) in DMSO-d_6 at RT.

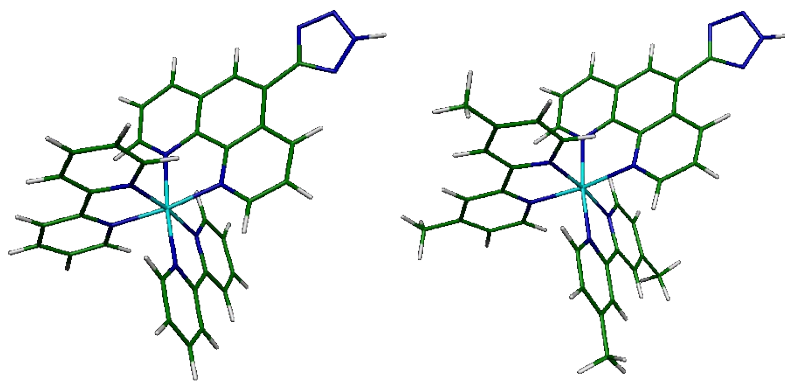
S3. DFT Calculations

The molecular and electronic structure calculations were performed with density functional theory (DFT) using the Gaussian 09 (G09) software package, employing the B3LYP exchange-correlation functional. The LANL2DZ and 6-31G* basis sets were used respectively for Ru and the ligands, and the LANL2 pseudopotential was used for the core electrons of Ru. All geometry optimizations were performed in either C1 or C2 symmetry with subsequent frequency analysis to show that the structures are at the local minima on the potential energy surface. The molecular orbitals were visualized using Gauss View 5.0.8.

Frontier molecular orbitals and the energy diagrams of SA1-SA3 are shown in below (Figure S8). In each complex, HOMO, HOMO-1 and HOMO-2 are located mainly at the Ru(II) atom. LUMO is delocalized mainly over the Tzphen and ancillary ligands. On the other hand, LUMO+1 of SA1 is delocalized mainly over the Tzphen and ancillary (bpy) ligands and LUMO+1 of SA2 and SA3 were delocalized over the Tzphen ligand. For SA1 and SA2, LUMO+2 were populated mainly at both the Tzphen and ancillary (bpy, dmbpy) ligands, and LUMO+2 of SA3 is delocalized mainly over the phen ligand.

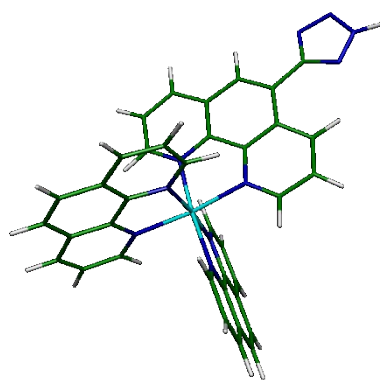
Time Dependent (TD) DFT calculations were performed on the optimized structures in order to simulate absorption spectra, using the B3LYP exchange-correlation functional within the Amsterdam Density Functional program package (ADF2014) [4-6]. We employed the spin-orbit (SO) ZORA Hamiltonian, in order to consider spin orbit coupling (SOC) effects. The

relativistic TDDFT formalism as implemented in ADF for closed-shell molecules, including SOC, is based on the ZORA two components Hamiltonian [7,8]. Relativistic spectra were evaluated taking into account the SOC in a self-consistent perturbative way [9]. The 12 lowest transitions were considered in each case. The absorption spectra were simulated by interpolating the computed transitions by Gaussian functions with a broadening $\sigma=0.075$, corresponding to an FWHM of 0.18 eV, thus matching the experimental one.



SA1

SA2



SA3

Figure S7 Optimized molecular structures SA1, SA2 and SA3.

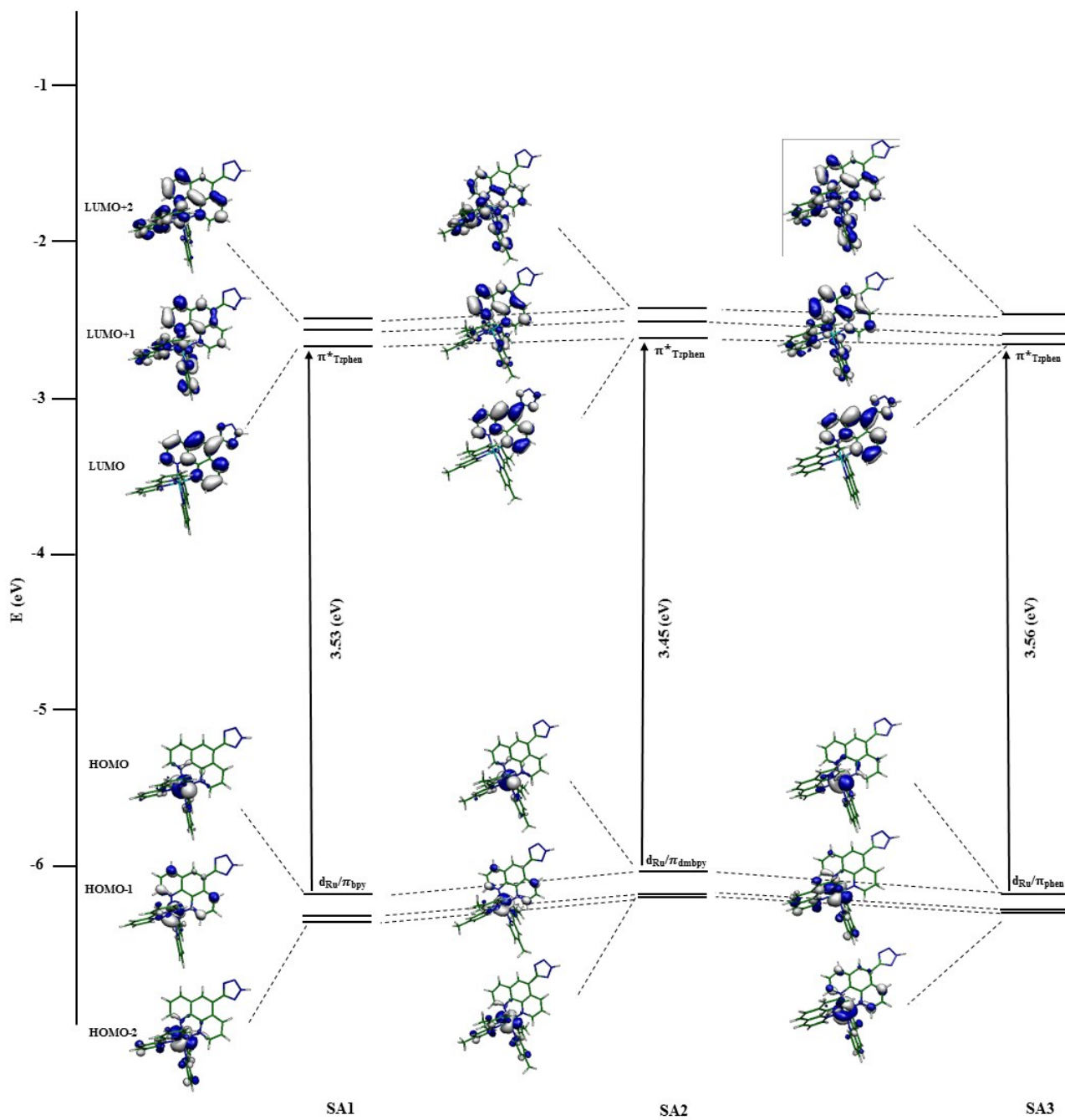


Figure S8. Isosurfaces for the HOMO and LUMO of complexes obtained from DFT method through LANL2DZ/ 6-31G* basis set.

Table S1. The energy levels complexes SA1, SA2 and SA3 calculated using LANL2DZ/6-31G* basis set in the solution phase based on the optimized S_0 geometries.

Complex	HOMO (eV)	LUMO (eV)	Band Gap
SA1	-6.16	-2.63	3.53
SA2	-6.04	-2.59	3.45
SA3	-6.18	-2.62	3.56

Table S2. First two triplet states for complexes SA1, SA2 and SA3 calculated using the TDDFT approach.

Complex	State (E, λ)	Assignment (HOMO= H, LUMO= L)	Character
SA1	T ₁ (2.7314 eV, 440 nm)	H→L (42%) H→L+2 (41%)	$d_{Ru}/\pi_{(bpy)2} \rightarrow \pi^*_{Tzphen}$ $d_{Ru}/\pi_{(bpy)2} \rightarrow \pi^*_{Tzphen}/\pi^*_{bpy}$
	T ₂ (2.7478 eV, 451 nm)	H→L+1 (13%) H→L+2 (42%)	$d_{Ru}/\pi_{(bpy)2} \rightarrow \pi^*_{Tzphen}/\pi^*_{(bpy)2}$ $d_{Ru}/\pi_{(bpy)2} \rightarrow \pi^*_{Tzphen}/\pi^*_{bpy}$
SA2	T ₁ (2.6495 eV, 468 nm)	H→L (39%) H→L+1 (48%)	$d_{Ru}/\pi_{(bpy)2} \rightarrow \pi^*_{Tzphen}$ $d_{Ru}/\pi_{(bpy)2} \rightarrow \pi^*_{Tzphen}/\pi^*_{(dmbpy)2}$
	T ₂ (2.7402 eV, 452 nm)	H→L+1 (37%) H→L+2 (50)	$d_{Ru}/\pi_{(bpy)2} \rightarrow \pi^*_{Tzphen}/\pi^*_{(dmbpy)2}$ $d_{Ru}/\pi_{(bpy)2} \rightarrow \pi^*_{Tzphen}/\pi^*_{(dmbpy)2}$
SA3	T ₁ (2.7565 eV, 450 nm)	H→L (40%) H→L+1 (43%)	$d_{Ru}/\pi_{(phen)2} \rightarrow \pi^*_{Tzphen}$ $d_{Ru}/\pi_{(phen)2} \rightarrow \pi^*_{(phen)2}/\pi^*_{Tzphen}$
	T ₂ (2.8205 eV, 440 nm)	H→L+2 (22%)	$d_{Ru}/\pi_{(phen)2} \rightarrow \pi^*_{(phen)2}/\pi^*_{Tzphen}$

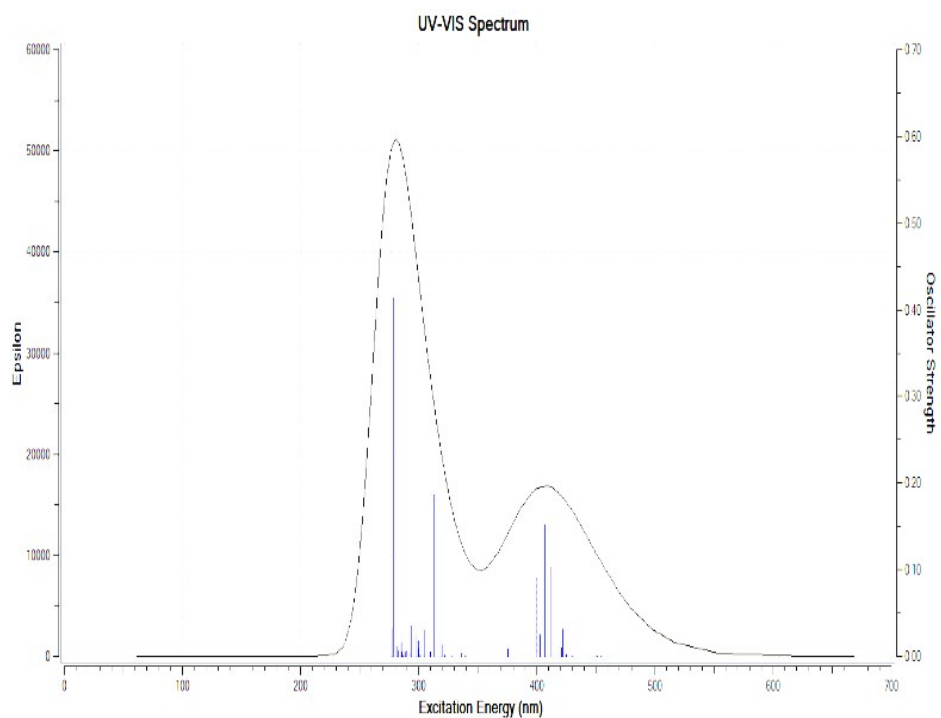


Figure S9. Simulated absorption spectrum of complex SA1 in dimethylformamide solvent.

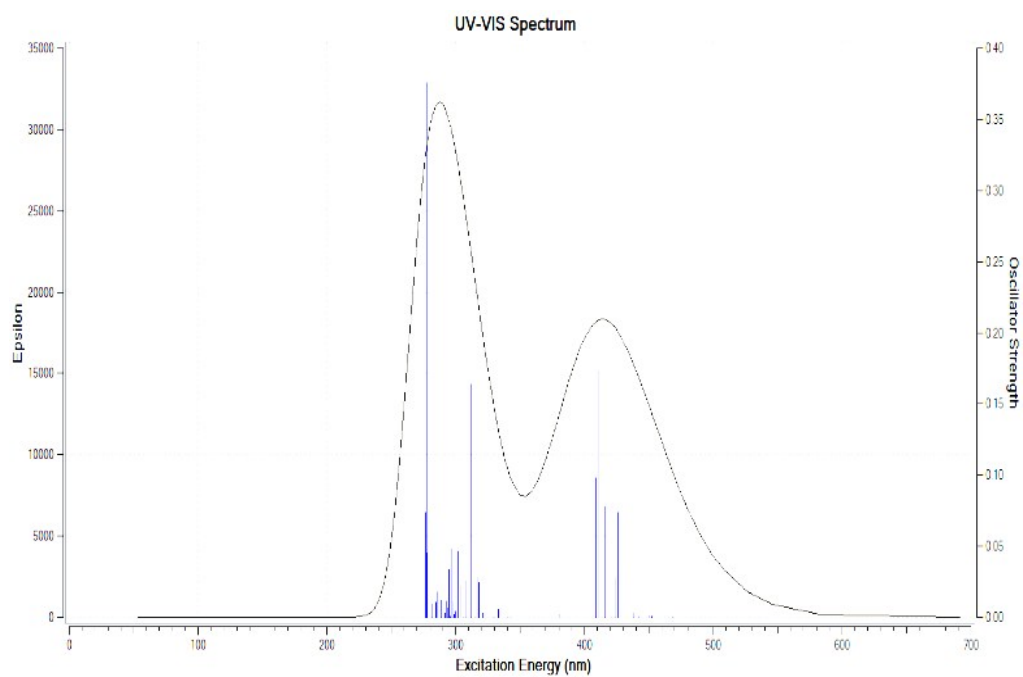


Figure S10. Simulated absorption spectrum of complex SA2 in dimethylformamide solvent.

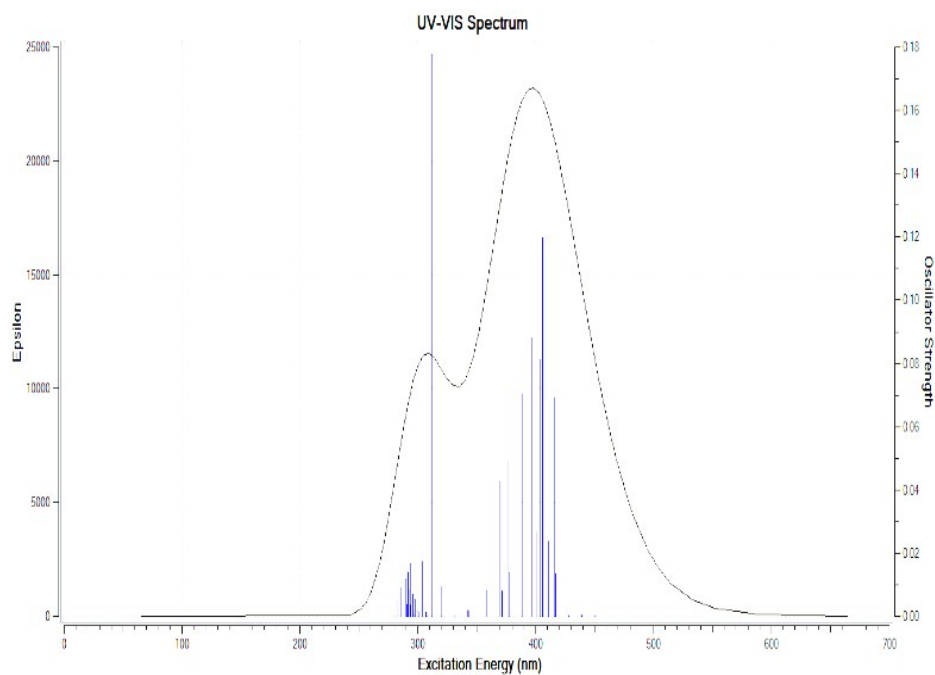


Figure S11. Simulated absorption spectrum of complex SA3 in dimethylformamide solvent.

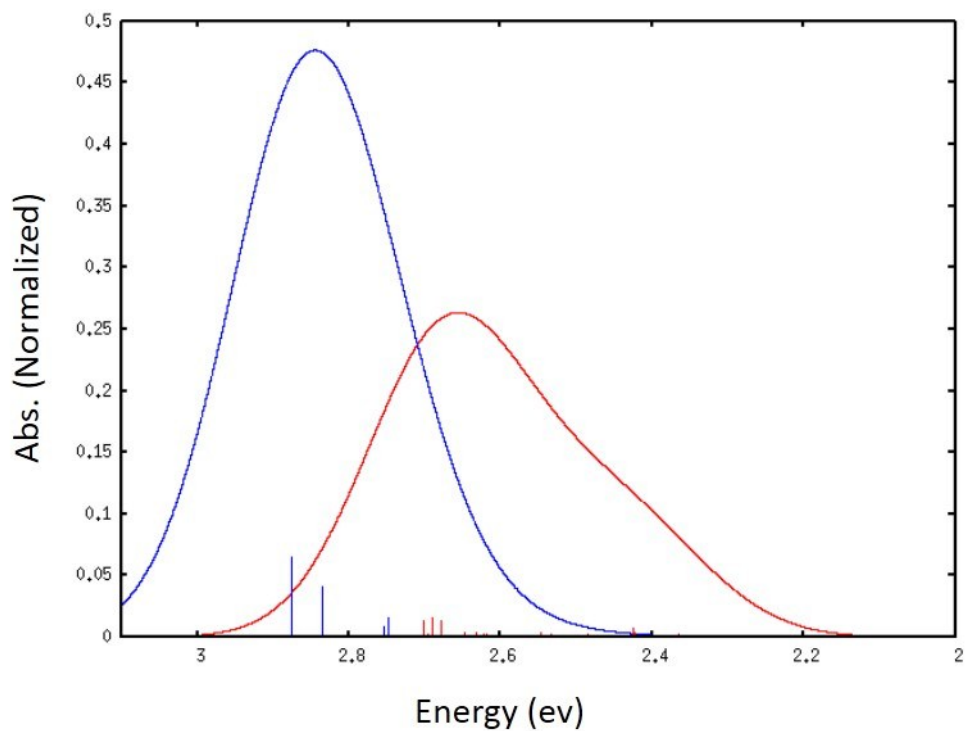


Figure S12. TDDFT calculated absorption spectra of SA1 with (red) and without (blue) spin-orbit coupling. Notice the broadening and red-shift of the absorption spectrum in the presence of spin-orbit coupling.

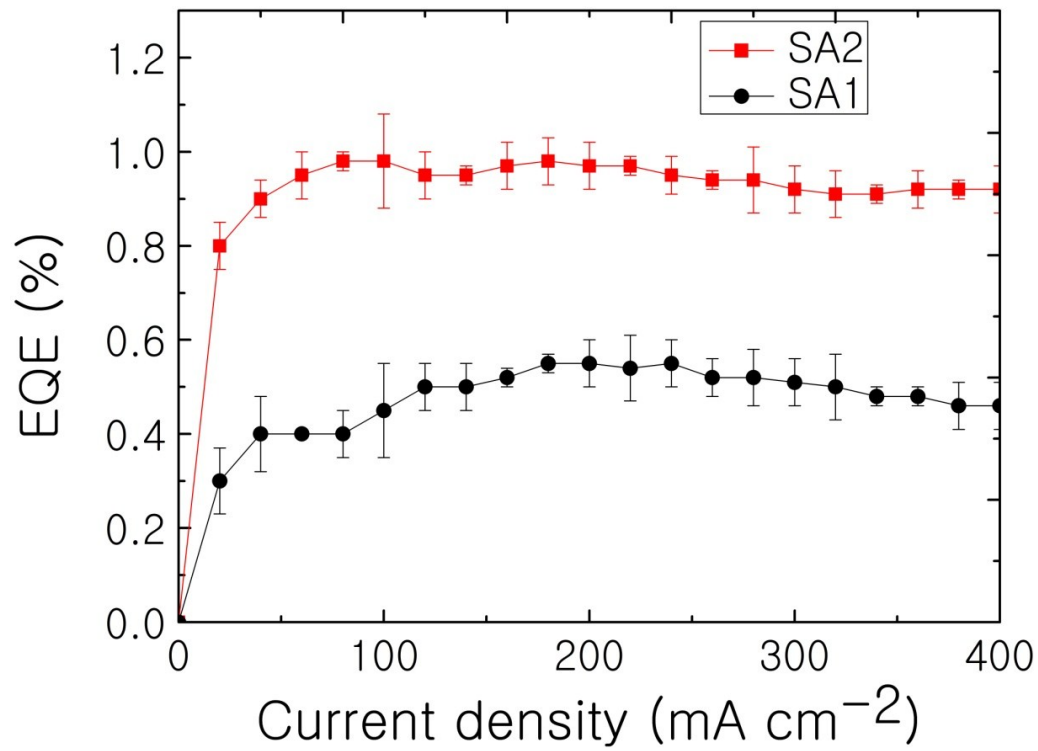


Figure S13. The EQE value over current density of SA1 and SA2.

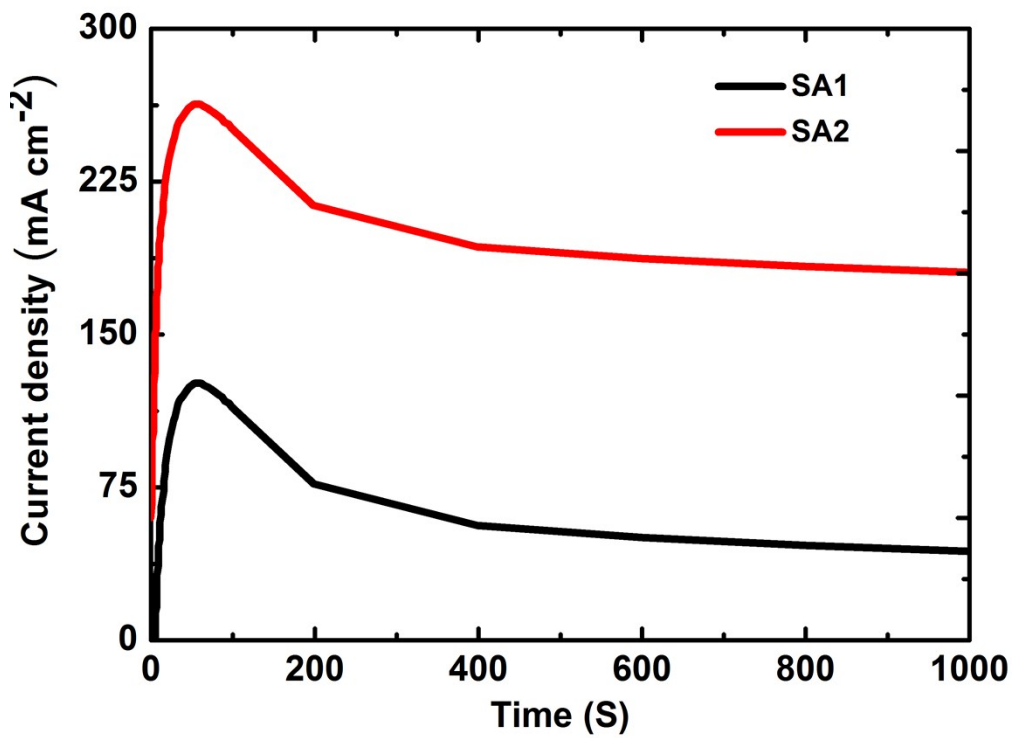
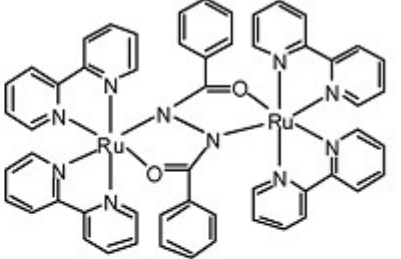
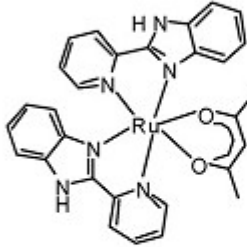
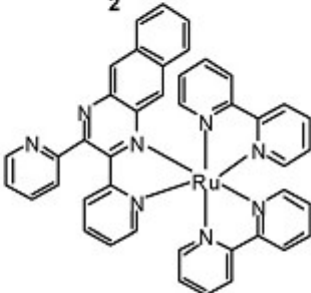
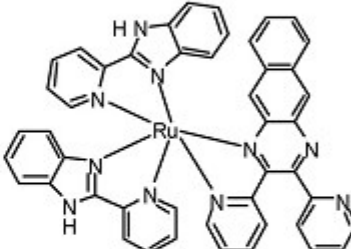
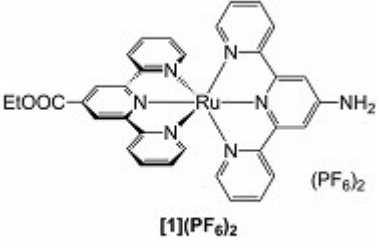
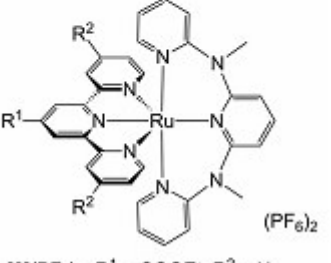
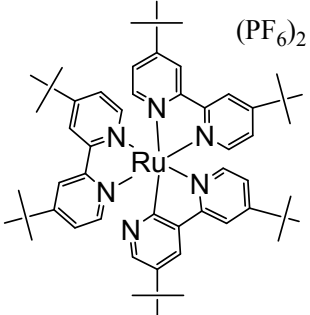
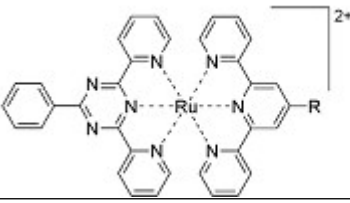


Figure S14. Current over time for LEC devices of ITO/[Ru tetrazole] /Ga:In/epoxy at an applied bias of 5 V.

Table S3. The molecular structures and EL properties of near infrared light electrochemical cell based on ruthenium polypyridyl complexes

Complexes	Cell configuration	EL _{max} (nm)	ext (%) η	Ref.
	ITO/complex (100 nm)/Au (100 nm)	630	0.31	(10)
	ITO/complex (100 nm)/Au (100 nm)	780	0.013	(10)
	ITO/complex (100 nm)/Au (100 nm)	880	0.075	(10)
	ITO/complex (100 nm)/Au (100 nm)	900	0.06	(10)
	ITO/complex (100 nm)/Au (100 nm)	945	0.03	(10)

		ITO/complex (100 nm)/Au (100 nm)	1040	-	(10)
 <p>[1](PF₆)₂</p>	ITO/PEDOT:PSS(45nm)/Ru:PMMA (169-194 nm)/Ag	733	0.001	(11)	
 <p>[2](PF₆)₂: R¹ = COOEt; R² = H</p>	ITO/PEDOT:PSS(45nm)/Ru:PMMA (169-194 nm)/Ag	722	0.028	(11)	
 <p>[3](PF₆)₂: R¹ = R² = COOMe</p>	ITO/PEDOT:PSS(45nm)/Ru:PMMA (169-194 nm)/Ag	745	0.013	(11)	
 <p>(PF₆)₂</p>	ITO/PEDOT:PSS(30nm)/Ru/Ag	600, 720	2.06, 0.27 (after 100 min)	(12)	
 <p>1: R=H</p>	ITO/PEDOT:PSS/complex:PMMA /Al	717	0.005	(13)	

	TO/PEDOT:PSS/ complex:PMMA /Al	725	0.005	(13)
---	--------------------------------------	-----	-------	------

References:

- [1] Kwon, Y.; Choe, Y.; Electroluminescent Properties of LECs Based on Ionic Transition Metal Complexes Using Tetrazole-Based Ancillary Ligand, *J. Sol. Chem.*, **2014**, 43, 1710–1721.
- [2] Shen, Y.; Sullivan B. P.; A Versatile Preparative Route to 5-Substituted-1,10-Phenanthroline Ligands via 1,10-Phenanthroline5,6-Epoxyde , *Inorg. Chem.* **1995**, 34, 6235-6236.
- [3] Zhang , W.; Zhao, Fei .; Liu , T.; Yuan , M.; Wang, Z. M.; and Gao, S.; Spin Crossover in a Series of Iron(II) Complexes of 2-(2-Alkyl-2H-tetrazol-5-yl)-1,10-phenanthroline: Effects of Alkyl Side Chain, Solvent, and Anion , *Inorg. Chem.*, **2007**, 46, 2541–2555.
- [4] te Velde, G. *et al.* Chemistry with ADF. *J. Comput. Chem.* **2001**, 22, 931-967.
- [5] Guerra, C. F., Snijders, J. G., Te Velde, G. & Baerends, E. J. Towards an Order-N DFT Method. *Theor. Chem. Acc.* **1998**, 99, 391-403.
- [6] ADF 2014, SCM (Theoretical Chemistry, Vrije Universiteit, Amsterdam, The Netherlands, 2014).
- [7] Visscher, L. & van Lenthe, E. On the Distinction Between Scalar and Spin-Orbit Relativistic Effects. *Chem. Phys. Lett.* **1999**, 306, 357-365.
- [8] Vanlenthe, E., Baerends, E. J. & Snijders, J. G. Relativistic Regular 2-Component Hamiltonians. *J. Chem. Phys.* **1993**, 99, 4597-4610.
- [9] Wang, F. & Ziegler, T. A Simplified Relativistic Time-Dependent Density-Functional Theory Formalism For The Calculations Of Excitation Energies Including Spin-Orbit Coupling Effect. *J. Chem. Phys.* **2005**, 123.

- [10] S, Xun.; J. Zhang.; X. Li.; D, Ma.; Z, Yuan Wang.; Synthesis and near-infrared luminescent properties of some ruthenium complexes , *Syn. Met.* **2008**, 158, 484–488.
- [11] A, Breivogel.; M, Park.; D, Lee,S, Klassen.; A, Kühnle.; C, Lee.; K, Char.; K, Heinze, Push-pull design of bis(tridentate) ruthenium(II) polypyridine chromophores as deep red light emitters in light-emitting electrochemical cells, *Eur. J. Inorg. Chem.***2014**, 288–295.
- [12] J-H, Hsu, H-C, Su.; Host-only solid-state near-infrared light-emitting electrochemical cells based on interferometric spectral tailoring, *Phys. Chem. Chem. Phys.*,**2016**,18, 5034—5039.
- [13] H, Bolink.;E, Coronado.; R, Costa.; P, Gavina.; E, Ortí.; S, Tatay.; Deep-red-emitting electrochemical cells based on heteroleptic bis-chelated ruthenium(II) complexes, *Inorg. Chem.* **2009**, 48, 3907-3909.